Toxicity of ceria nanoparticles to the regeneration of freshwater planarian Dugesia japonica

Xie, Changjian; Li, Xiaowei; Hei, Lisha; Chen, Yiqing; Dong, Yuling; Zhang, Shujing; Ma, Shan; Xu, Jianing; Pang, Qiuxiang; Lynch, Iseult; Guo, Zhiling; Zhang, Peng

DOI:
10.1016/j.scitotenv.2022.159590

Document Version
Peer reviewed version

Citation for published version (Harvard):
Xie, C, Li, X, Hei, L, Chen, Y, Dong, Y, Zhang, S, Ma, S, Xu, J, Pang, Q, Lynch, I, Guo, Z & Zhang, P 2023, 'Toxicity of ceria nanoparticles to the regeneration of freshwater planarian Dugesia japonica: The role of biotransformation', *Science of the Total Environment*, vol. 857, 159590.
https://doi.org/10.1016/j.scitotenv.2022.159590

Toxicity of ceria nanoparticles to the regeneration of freshwater planarian Dugesia japonica: the role of biotransformation

Changjian Xie [a,], Xiaowei Li [a], Lisha Hei [a], Yiqing Chen [a], Yuling Dong [a], Shujing Zhang [a], Shan Ma [d], Jianing Xu [a], Qiuxiang Pang [a,*], Iseult Lynch [b], Zhiling Guo [b,*], and Peng Zhang [b, c]*

[a] *School of life Sciences and medicine, Shandong University of Technology, Zibo 255000, Shandong, China*

[b] *School of Geography, Earth & Environmental Sciences, University of Birmingham, Edgbaston, Birmingham B15 2TT, United Kingdom*

[c] *Department of Environmental Science and Engineering, University of Science and Technology of China, Hefei 230026, China*

[d] *Zibo Environment Monitoring Center, Zibo25500, Shandong, China*

** Corresponding authors:*

E-mail addresses: xiecj@sdut.edu.cn (Changjian Xie), pangqiuxiang@sdut.edu.cn (Qiuxiang Pang), z.guo@bham.ac.uk (Zhiling Guo).

Abstract

Cerium oxide nanoparticles (n-CeO_2) have wide applications ranging from industrial to consumer products, which would inevitably lead to their release into the environment. Despite the toxicity of n-CeO_2 on aquatic organisms has been largely reported, research on developing organisms is still lacking. In this study, we investigate the toxic effects of n-CeO_2 on the stem cells, tissue- and neuro-regeneration, using freshwater planarian *Dugesia japonica* as a model. Effects of bulk sized (μ-) CeO_2 and ionic Ce (Ce^{3+}) were compared with that of n-CeO_2 to explore the origin of the toxic effects of n-CeO_2. No overt toxicity was observed in μ-CeO_2 treatment. n-CeO_2 not only impaired the homeostasis of normal planarians, but also inhibited the regeneration processes of regenerated planarians, demonstrated by the inhibited blastema growth, disturbed antioxidant defense system at molecular levels, elevated DNA-damage and decreased stem cell proliferation. Regenerating organisms are more susceptible to n-CeO_2 than the normal ones. Ce^{3+} exhibited significantly higher toxicity than n-CeO_2, even though the total Ce uptake is 0.2% less in Ce^{3+} than in n-CeO_2 treated in planarian. X-ray absorption near edge spectroscopy (XANES) analysis revealed that 12.8% of n-CeO_2 (5.95 mg/kg Ce per planarian) was transformed to Ce^{3+} after interaction with planarian, suggesting that biotransformation at the nano-bio interface might play an important role in the observed toxicity. Since the biotransformation of n-CeO_2 is a slow process, it may cause long-term chronic toxicity to planarians due to the slow whilst sustained release of toxic Ce^{3+} ions.

Keywords: n-CeO_2, toxicity, planarian, XANES; Regeneration

1. Introduction

The rapid development of nanotechnology promotes the applications of nanomaterials in various fields. Worldwide, about 10, 000 metric tons of cerium oxide nanoparticles (n-CeO_2) are produced per year[1]. n-CeO_2 are used in numerous applications such as biomedical fields, fuel additives, gas sensors, polishing agent, and metal-oxide semiconductor devices[2, 3]. The increasing production and widespread application would inevitably lead to the release of n-CeO_2 into the environment, causing concerns for the potential toxicological risks to aquatic organisms as well as human health[4]. Developing organisms and tissues are often more susceptible to environmental pollutants including nanoparticles[5].

The bio-effects of n-CeO_2 remain controversial. On one hand, n-CeO_2 is reported to have

inherent or acquired ability to scavenge reactive oxygen species (ROS)[6-8], which was equivalent to the antioxidant enzymes in biological systems[7, 9]. For example, n-CeO_2 can induce the proliferation of stem cells of mouse[10] and human[11] by regulating the intracellular ROS and the relative expression of genes responsible for the stem cell proliferation, migration and antioxidant defense system. Singh, et al. [12] also confirmed that n-CeO_2 can scavenge ROS accumulation and regulate the status of cell redox and thereby accelerating the growth in human keratinocytes (HaCaT cells). On the contrary, studies also showed that n-CeO_2 could exhibit adverse effects both *in vivo* and *in vitro*[13-15]. For instance, n-CeO_2 induced ROS accumulation and caused oxidative stress in *Caenorhabditis elegans* at environmental relevant concentration (1 nM), and ultimately led to a decreased lifespan[13]. The toxicity of n-CeO_2 depends on the species, dose, and the physiochemical property of n-CeO_2[14, 16-20]. The biological fates of n-CeO_2 are still unclear. Some studies suggest that the primary bioavailable form of n-CeO_2 in tissue is particulate form rather than the ionic (Ce^{3+}) [21] as n-CeO_2 was considered as highly insoluble under environmental conditions[22]. Studies based on synchrotron radiation techniques have revealed the biotransformation of n-CeO_2 in plants and bacteria[23-25]. Is the transformed n-CeO_2 responsible for the toxicity? This issue needs to be urgent studied.

Developing organisms and tissues are often more susceptible to environmental pollutants than mature organisms[26, 27]. Stem cells, which undergo rapid cell division, are highly vulnerable to environmental chemicals, impairing their differentiation and development[28]. However, vertebrate experimental protocols need to be more prepared in terms of licensing and ethics. In fact, planarian as an alternative invertebrate organism has been proven to be an excellent stem cell model for more than 20 years[29]. Planarian has large numbers of pluripotent stem cells (20-30%) and can regenerate any body part including the whole head and the entire central nervous system[30], which makes them a suitable model for studying developmental (neuro-) toxicity[31]. In addition, planarian can provide early warning of harmful substances even at very low concentrations, thus, it is widely used as an indicator for water quality[5, 32]. As a benthic animal in the water body, planarians use their motile cilia to glide over sediment surfaces[33] and interacted with the deposited nanoparticles (NPs), which may make them an excellent model for investigating the effects of NPs on aquatic animals.

Planarians have been used for assessing nanotoxicity of Ag nanoparticles[5], polystyrene microplastics[34, 35], and Fe_3O_4 nannoparticles[36]. For instance, Kustov, et al. [37] found that Ag NPs was moderately toxic to the planarian with a dose-dependent effect. Compared with regeneration

planarians, the behavioral changes such as side-lying and screw-like movements, was only happened at the highest concentration (50 mg/L) in the homeostatic planarians, while the stem cell proliferation was not affected[5]. In a previous study, Fe_3O_4 NPs had not affected the stem cell population dynamics, nor did they induce significant changes in either homeostatic or regenerative planarians[36]. Instead, Ermakov, et al. [38] found that CeO_2 NPs (an average size of 1-2 nm) may play an inorganic mitogens role in stimulating *Schmidtea mediterranea* (planarian) regeneration at 10^{-11} M colloid solution, and CeF_3 NPs (F^- can stabilize Ce^{3+}that makes Ce^{3+} less prone to oxidation, $Ksp=8\times10^{-16}$ of CeF_3) also did not show any toxic to the homeostatic and regeneration planarians[39]. In fact, the toxicity of n-CeO_2 is related to its physicochemical properties, such as size, shapes, concentrations, Ce^{3+} released and species-specific. However, only little is known about the effects of n-CeO_2 sizes, doses, and biotransformation on the (neuro-) development toxicity of the aquatic organisms. In this study, we studied the toxicity of n-CeO_2 to freshwater planarian *Dugesia japonica* and compared their toxic effects to bulk-CeO_2 (μ-CeO_2), ionic Ce (Ce^{3+}) and control treatment (CT) on stem cells, tissue regeneration and development *in vivo*. We also used X-ray absorption near-edge spectroscopy (XANES) to identify the chemical species to examine the role of biotransformation in the observed biological effects.

2. Materials and Methods

2.1 Chemical and animals. n-CeO_2 (nominal size < 25nm, determined by nitrogen sorption, purity 99.9%, manufacturer's data) were purchased from Sigma-Aldrich (St. Louis, MO, USA). As previously reported[40], the particles were 100% cubic ceria with diameters ranging from 6.2 nm up to 48 nm, with the center of the distribution at 16.3 nm. The diameters of μ-CeO_2 (nominal size ＜5 μm, 99.9% trace metal basis, Sigma-Aldrich) varied from 237.5 nm to 1320 nm, and the distribution center was 473.5 nm (**Fig. S1**). Hydrodynamic size of n-CeO_2 and μ-CeO_2 in DI water and MW medium were 138.2 ± 31.8 nm and 2703.4 ± 147.6 nm, 162.3 ± 42.5 nm and 2863.2 ± 258.7 nm respectively. The zeta potential were 13.8 ± 4.0 mV and 11.5 ± 5.7 mV in DI water and 11.3 ± 2.9 mV and 9.8 ± 3.2 mV in MW medium for n-CeO_2 and μ-CeO_2 respectively. Cerium (III) chloride (CAS no. 7790-86-5, > 99.99%) was also purchased from Sigma-Aldrich.

Planarians *D. japonica* used in the study were collected from a spring in Yiyuan (Zibo, China), and acclimated in mineral water (MW, Lushan fountain water, Zibo, China) in a 12h/12h day/night

cycle at 20 ℃ for about 2 months to allow reproduce asexually in the laboratory. Then the planarians were maintained in our lab under the same cultural conditions for further studies. The planarians used in this study have been maintained in the lab for more than 1 year. Before exposure, the planarians were fed twice a week with bovine liver homogenate and the water was changed regularly (every two days) to ensure a clean environment. Planarians with lengths of 8 ~10 mm were selected for experiments and starved for at least a week before use.

2.2 Exposure experiment. Both homeostatic and regenerating planarians were used to examine the toxicity of n-CeO_2. Regeneration was induced right before exposure by transversally cutting homeostatic planarians anterior to the pharynx (mouth part) using an ethanol-sterilized razor blade, creating a head-regeneration part. Tissue regeneration, such as new blastema formation was monitored over time, indicated as days post amputation (dpa). Stock of n-CeO_2 (10 mg/mL), μ-CeO_2 (20 mg/mL) and Ce^{3+} (1000 mg/L) were prepared. *D. japonica* was exposed to different treatments for 7 days. MW medium was used as a control treatment. In brief, thirty planarians were exposed to 10 mL of each Ce-based material suspension with 3 replicates for each treatment. A series of n-CeO_2 suspensions (0.01, 0.1, 1, 10, 50, 100, and 200 mg/L), μ-CeO_2 suspensions (1, 10, 50, 100, 200, 500, and 1000 mg/L), and Ce^{3+} ions suspensions (0.01, 0.1, 0.5, 1, 5, 10, and 50 mg/L) were prepared in MW medium (the truth concentration was also detected by ICP-MS, **Table. S1**). The suspensions were sonicated in the MW medium for 15 mins before exposure. All experiments were performed in a 12h/12h day/night rhythm at 20 ºC. No food was given during the experiment. For homeostatic and regeneration planarians, the number of live planarians was recorded every day. Besides, based on acute toxicity tests, 40 mg/L n-CeO_2, 40 mg/L μ-CeO_2, and 3 mg/L Ce^{3+} were chosen for the follow-up studies as these concentrations were close to LC_{50} based on our preliminary experiment (**Fig. S2)**.

2.3 Phenotype assay For the regenerating planarians, the growth of the regeneration bud (blastema) was evaluated by measuring the size using a computer morphometry as described previously[41]. The planarians were photographed with a Nikon SMZ 1500 stereomicroscope (Nikon, Japan) at 7 dpa. The area of the blastema and the total area of the body were determined using Image J software (Version 1.8.0, Wayne Rasband, National Institutes of Health, Bethesda, MD, USA). The quantitative measure of blastema growth was calculated as the values of new blastema size divided by the sizes of the whole body were used as. Data from 30 animals were averaged. All experiments at each time

point were repeated in triplicate. Each planarian was photographed at the same exposition and magnification. Details of the experiments are shown in the **SI**.

2.3 Post-exposure locomotion velocity (*pLMV*) assay. At 7 dpa, thirty planarians per treatment were individually placed in the center of a clear acrylic box (50.0 cm × 50.0 cm) positioned over graph paper (grid lines spaced 0.5 cm apart) with mineral water covering the bottom of the paper. The observation started 30 s after placement of the planarians at the center of the grid and lasted for 8 min. *pLMV* was measured as the number of grid lines that each planarian crossed or re-crossed per min over an 8 min observation period.

2.4 Whole-mount *in situ* hybridization (WISH). After 2 days of exposure to Ce-based suspensions, the regenerated planarians (2 dpa) were used for *in situ* hybridizations. The experiments were performed to characterize the expression level of *Djpiwi-A*, which is the main stem cell marker gene[42] following a previously described method[43]. In brief, *Djpiwi-A* probe primers (F: 5'-AAGAGAGATAGGAAGACTGCG-3' and R: 5'-GATCACTAATACGACTCACTATAGGGAAGAGAGATAGGAAGACTGCG-3') were designed, synthesized and labeled with digoxigenin (DIG) using an *in vitro* labeling kit (Roche, Switzerland). Planarians were then analyzed using a stereomicroscope (Nikon, SMZ1500, Japan). Each planarian was photographed at the same exposition and magnification. Details of the experiments are shown in the **SI**.

2.5 Whole-mount immunofluorescence. At 2 dpa, 30 planarians were collected for immunochemistry following a previously described method[44]. Anti-phospho-histone-3 (H_3P, Millipore, Billerica, MA, USA) was used at a 1:500 dilution to investigate the effects on the stem cell proliferation (*in vivo* mitotic activity of stem cells). Phospho-histone-3-positive cells were counted under an Olympus DP80 inverted microscope (Olympus, Tokyo, Japan). To analyze differences in the regeneration of the center nervous system (CNS), immunostaining was carried out using anti-SYNORF1 (3C11, mouse monoclonal antibody specific for synapsin, 1:500 dilution) to investigate the effects on the neurodevelopmental process, and nerve fiber density of SYNORF1-immunopositive neurons were measured at 10 dpa. The detailed method is shown in the **SI**.

2.6 ICP-MS and XANES measurement. To quantify the concentration of Ce in the regenerating planarians, the samples were collected at 2 dpa after a thorough wash using DI water. For ICP-MS

analysis, these samples were freeze-dried, ground into fine powders and digested with a 3:1 (*v*:*v*) mixture of HNO_3 (75%) and H_2O_2 (25%) on a heating plate (80 °C for 1 h, 120 °C for 3 h, and 160 °C for 0.5 h). Ce concentrations in the digestion solution were then analyzed by inductively coupled plasma-mass spectrometry (ICP-MS, 7900, Agilent Technologies). Ce standard solutions (0.5-50 mg/L) were used for calibration. The recovery rate of Ce was tested to be 99.75%.

XANES was used to quantify the Ce^{3+} fraction in the regenerating planarians. At 2 dpa, the planarians were collected, freeze-dried, motor-homogenized, and pressed into circulars slices with a diameter of 10 mm and a thickness of 1 mm. Fluorescence mode was applied for the collection of Ce L_{III}-edge XANES spectra of the samples and reference standards. Athena software was used to perform liner combination fitting (LCF analysis) of XANES spectra[45].

2.7 Oxidative Stress responses. At 2 dpa, 30 planarians were collected and homogenized in PBS on ice using a tissue grinder (Tiangen, OSE-Y20, Beijing, China) with a pestle (Tiangen, OSE-Y001, Beijing, China). The homogenates were centrifuged at 12,000 *g* at 4 ℃ for 10 min. The supernatant was collected for determination of activities of superoxide dismutase (SOD), glutathione peroxidase (GPx), and glutathione S-transferase (GST) and contents of malondialdehyde (MDA), glutathione (GSH), and glutathione disulfide (GSSG) following the manufacturer's instructions. Details of the analyses are provided in the **SI**.

At 2 dpa, 10 planarians for collected for real-time quantitative PCR analysis (qPCR). Total RNA was isolated using TRIzol (Invitrogen, USA). cDNAs were generated from total RNA with the reverse transcription system (Thermo, USA). The expression of oxidative stress-associated genes (*gpx*, *gst, p53* and *nak*) in planarians were quantified (LightCycler 480 II Real-Time PCR System (Roche, Basel, Switzerland)). The primer sequences are provided in **Table S3**. The detailed method is shown in the **SI**.

2.8 ELISA for Caspase-3 and 8-OHdG activities. At 2 dpa, 5-6 planarians were collected for ELISA. Cleaved cysteine-aspartic proteases-3 (caspase-3), an apoptotic marker, was quantified in planarian's tissue using a commercially available ELISA assay (Jiangsu Jingmei Biotechnology Co., Ltd, Jiangsu, China). The content of 8-hydroxy-2 deoxyguanosine (8-OHdG) was measured to assess the oxidative damage to DNA using a DNA Damage ELISA kit (Jiangsu Jingmei Biotechnology Co., Ltd, Jiangsu, China). Details of sample preparation and the analyses are shown in the **SI**.

2.9 Statistical analysis. All tests were repeated at least three times. Data were expressed as mean ±

SD (standard deviation). Statistical significance was analyzed by ANOVA or student's t-test. $p < 0.05$ was considered as the level of significance.

3. Results and discussion

3.1 Effect of n-CeO_2 exposure on tissue regeneration and mobility of regenerating planarian

A pilot experiment was carried out to identify the exposure concentration (**Fig. 1a**). As shown in **Fig. S2** and **Table. S4-S5**, the LC_{50} values after 7-day n-CeO_2 exposure for homeostatic and regeneration planarians were 51.2 mg/L and 46.3 mg/L, respectively. The LC_{50} of Ce^{3+} for the homeostatic and regenerating groups were 3.5 mg/L and 3.2 mg/L, respectively (**Table. S4-S5**). Therefore, we chose 40 mg/L n-CeO_2, 40 mg/L μ-CeO_2, and 3 mg/L Ce^{3+} which were close to the LC_{50} values for the following studies.

After an injury, the stem cells (neoblasts cells) in the planarian would proliferate and migrate to the wound site to form a protective mass of new cells which called blastema[46]. We examined the influences on the tissue regeneration by measuring the size of newly growing blastema after decapitation. As shown in **Fig. 1b** and **1c**, the average anterior new blastema sizes in the n-CeO_2 and Ce^{3+}-exposed planarians were significantly smaller than CT and μ-CeO_2 groups. In the CT and μ-CeO_2 groups, 100% planarians developed eyes at the 7 dpa, whereas only 12.5% and 6.7% of planarians reformed eyes under n-CeO_2 and Ce^{3+} ions exposure, respectively (**Fig. 1d**). These results indicated that the n-CeO_2 and Ce^{3+} treatment delayed planarian's regeneration. Locomotion velocity test result showed that n-CeO_2 and Ce^{3+} reduced the mobility of the regenerating planarians (**Fig. 1e**). The data were plotted as the cumulative means of each group over an 8-min observation period at 7 dpa. The slope of the plot represents the speed of movement across the gridlines. The planarians in the CT group displayed an average *pLMV* of about 18.3-24.3 gridlines per minute (the slope value is 20.1), similar to that of the μ-CeO_2 group (the slope value is 17.8). n-CeO_2 and Ce^{3+} ions reduced the slope of the *pLMV* to 8.9 and 3.8, respectively.

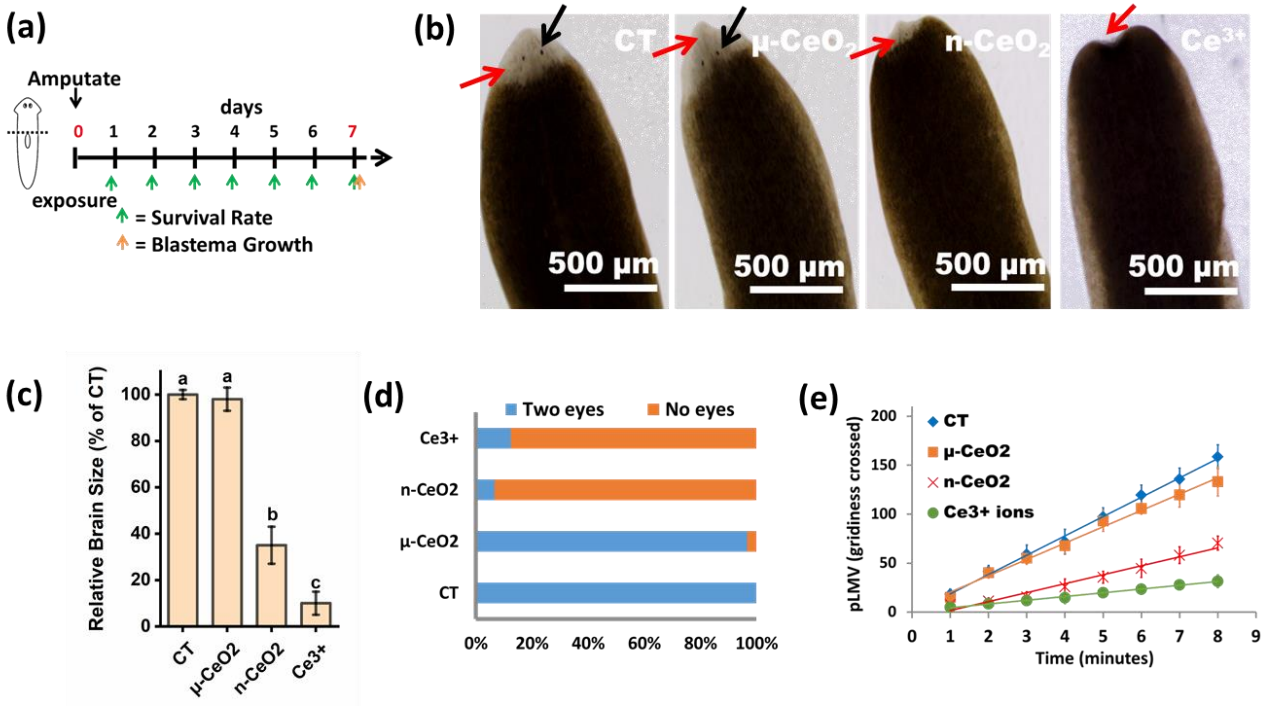

Fig. 1 n-CeO_2 and Ce^{3+} delay planarian regeneration and affect the mobility. **a**) Experimental time points of Ce-based suspensions (40 mg/L n-CeO_2, 40 mg/L μ-CeO_2, and 3 mg/L Ce^{3+}) exposure, amputation, and morphological observation. **b**) Blastema reform at 7 dpa in different treatments (**Black Arrow**: eyespots; **Red Arrow**: blastema). **c**) Average size of regenerated blastema in proportion to the body area of the planarian. **d**) Percentage of planarians with eyespots regeneration in different treatments. **e**) Effect of Ce-based suspensions on the regenerating planarians' motility at 7 dpa. *PLMV* was quantified as the number of gridlines crossed or re-crossed over an 8-min. This was plotted as cumulative crosses vs. time. Thirty animals per experimental condition were used, and each experiment was repeated three times. The results are presented as the mean ± SD, one-way ANOVA.

3.2 n-CeO_2 impaired stem cell dynamics and regeneration of the nervous system.

The stem cell proliferation promotes the tissue regeneration. Planarian has large number of pluripotent stem cells for rapid cell division and regeneration. The decreased size of anterior new blastema may arise from the disrupted cell division and regeneration. Stem cells are highly vulnerable to environmental chemicals, which can lead to adverse effects on differentiation processes and development[47]. The detailed experimental design was described in **Fig. 2a**. *DjpiwiA*, a main stem cell gene marker[44], was quantified using the WISH method. As shown in **Fig. 2b**, at 2 dpa, *DjpiwiA* were extensively expressed (shown as the blue color) in the whole body except for the pharynx in CT and μ-CeO_2 group, and the expression were reduced by 29.2% and 38.4% in n-CeO_2 and Ce^{3+}group, respectively.

During development, mitotic activity (cell proliferation) can be regarded as one of the primary

events of tissue remodeling and repair[48]. Anti-phospho-Histone H3 antibody can be used to label the nuclei of stem cells to examine the in *vivo* mitotic activity[49]. Compared to CT group, the number of labeled nuclei (green dots) significantly decreased by 63.1% and 65.2% after exposure to n-CeO_2 and Ce^{3+}, respectively (**Fig. 2c**), while μ- CeO_2 group did not show significant difference with CT. This suggested that n-CeO_2 and Ce^{3+} treatment impaired the proliferation of stem cell.

A recent study found that Ag NPs can affect the locomotion of freshwater planarians *Schmidtea mediterranea* by inducing neurotoxicity and disorder in neurodevelopment[5]. These suggested that n-CeO_2 induced locomotive inhibition may be attributed to the neurotoxicity. Planarian is a unique in the animal kingdom as they can regenerate its brain, including a fully functional CNS[50]. To evaluate whether the reduced stem cell proliferation further impeded the regeneration of the CNS, the neuron morphologies were observed at 10 dpa using immunohistochemistry method. The anti-SYNORF1 antibody was used as a biomarker, which allows visualization of the planarian CNS. The normal planarian brain has an inverted U-shaped structure comprised of a cortex of neural cells and a core of axons, which displays rich branches[51]. Based on the behavioral changes and regeneration defects, we observed that planarian could not regenerate its complete CNS. As shown in **Fig. 2d**, n-CeO_2 and Ce^{3+} treatment significantly reduced the number of lateral branches, indicating that n-CeO_2 and Ce^{3+} induced neural regeneration defects in the treated planarians. μ-CeO_2 groups showed no significant effect. Overall, these results suggest that n-CeO_2 and Ce^{3+} exposure impaired the stem cell activity and neurodevelopment, and thus the health and regeneration capacity of the CNS in the exposed planarians.

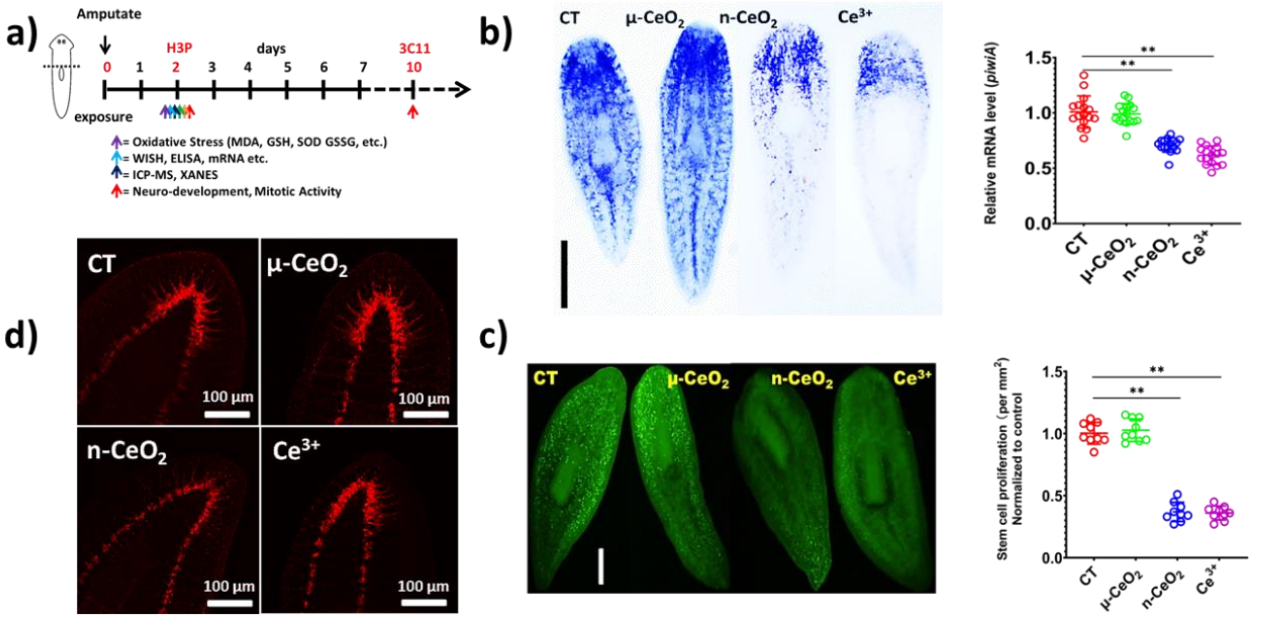

Fig. 2 n-CeO_2 and Ce^{3+}affects stem cell proliferation. (**a**) Experimental time points of Ce-based suspensions (40 mg/L n-CeO_2, 40 mg/L μ-CeO_2, and 3 mg/L Ce^{3+} ions) exposure to regeneration planarians and detect biomarkers, such as oxidative stress marker MDA and SOD, WISH and Immunochemistry. (**b**) **Left**, *in situ* hybridization to detect *DjpiwiA* transcripts in planarians. **Right**, the gene expression of *DjpiwiA* in the regenerating planarians in different treatment. (**c**) Immunohistochemistry using the mitotic marker Anti-H_3P antibody. The **left** panel shows a view of the mitotic cells in regenerating planarian in different treatments. **Right**, the number of mitotic events in Ce-based suspensions treatment and control (**CT**) groups. The results are presented as the mean ± SD of a minimum of 10 biological replicates per condition (1 planarian per point, asterisks indicate the level of significant differences between treatment and CT groups of the planarian, one-way ANOVA, *$p < 0.05$ **$p < 0.01$). (**d**) Whole-mount immunostaining of the nervous system with anti-SYNORF1 (3C11) in regeneration planarians after exposure to Ce-based suspensions for 10 days. Scale bars represent 2 mm or 100 μm.

3.3 Chemical origin of the toxicity: role of bioaccumulation and biotransformation

Biotransformation and bioaccumulation determine the ultimate fate and toxicity of nanomaterials in living organisms[52, 53], such as *Lactuca plants*[39], *Bacillus subtilis*[24], and *Chlorella pyrenoidosa*[14]. *In vivo* studies rarely consider physicochemical characteristics and actual exposure concentrations when linking them to uptake, distribution patterns, and potential adverse effects. In the present study, the actual size of the n-CeO_2 and μ-CeO_2 were considerably larger than their nominal reported size (**Fig. S3**). In fact, n-CeO_2 and μ-CeO_2 changes in both concentration and particle size were observed during the exposure concentration (**Fig. S4**, the hydrodynamic diameter from 162 nm and 2863 nm at the beginning up to 312 nm and 3312 nm at 48 h by n-CeO_2 and μ-CeO_2 interacted with planarian, respectively; **Table S6**). Sedimentation also depends on the surrounding environment[5], such as the production of organic material mucus, in which particles agglomerate (**Fig.S4-S5**). This way, the bioavailability in the aquatic column is reduced, while increasing the risk for benthic animals.

Planarians inhabit the lowest water layer, and are able to take up NPs as they glide over the substrate[5]. Then we used ICP-MS to detect the Ce-based materials and found that Ce was significantly accumulated in the regeneration planarian after 2 days of exposure to different Ce treatments, and n-CeO_2 group showed the highest accumulation, followed by μ-CeO_2 and Ce^{3+} group (**Fig. 2b**). For the 40 mg/L μ-CeO_2, n-CeO_2, and 3 mg/L Ce^{3+} ions, Ce accumulations in the planarians were 27.6±4.7, 46.5±7.8, and 2.8±0.4 mg Ce kg^{-1}, respectively. The percentages of the accumulation from the total applied Ce are 0.31%, 0.52% and 0.32% for μ-CeO_2, n-CeO_2 and Ce^{3+}, respectively. Many factors would influence the bioaccumulation and bioavailable of Ce in planarian, such as sizes and culture environment. On the one hand, n-CeO_2 with smaller size is easier to move into the organism thus accumulate more than μ-CeO_2. For example, neither μ-CeO_2 nor n-CeO_2 are ingested by planarian, however, the latter with a smaller size allows them to stay a longer time in body during this ingestion process. In addition, planarians use their motile cilia to glide across the sediment surface and come into contact with the deposited materials, which make them adsorb μ-CeO_2 and n-CeO_2 in their body. Besides, planarian will secrete mucus after being stimulated, as shown in **Fig. S5**, large numbers of mucus proteins were present in the n-CeO_2 treatment group while a small amount these proteins were present in the μ-CeO_2 group, which may promote n-CeO_2 adsorption by planarian. Once n-CeO_2 penetrated into glial and neurons cells, it would be directed to the lysosomes or persist in the cytoplasm and subsequently interact with other organelles[54]. Although μ-CeO_2 also accumulated significant amount of Ce (equal to 60% of that in n-CeO_2 group), it did not show significant effects on locomotion, regeneration and neurodevelopment of planarian. Therefore, both the higher accumulation of Ce and higher reactivity of n-CeO_2 may contribute to its higher toxicity than μ-CeO_2. However, n-CeO_2 exposure resulted in 16.6-fold higher Ce accumulation but led to less toxicity than Ce^{3+}, further demonstrating that Ce^{3+} is more toxic than n-CeO_2. It is well known that nanomaterials in environment and biota may undergo transformation either through chemical or biological processes, and the transformation process may determine their toxicity[24, 55]. We therefore hypothesize that the biotransformation of n-CeO_2 might contribute to the significant toxicity.

We firstly examined the release of Ce^{3+} from μ-CeO_2 and n-CeO_2 in the culture media. Only less than 26.5 μg/L of Ce were detected, suggesting toxicity is unlikely caused by the Ce^{3+} that were initially in the exposure solution. However, biotransformation is a continuous process once the nanomaterials contact the biota[56]. Biotransformation of n-CeO_2 may occur on or within the planarian

during the exposure. Therefore, we examined the real amount of transformation in the organism using synchrotron radiation based XANES technique (**Fig. 3b**, **Table. S7**). The spectrum of Ce in the planarians under treatments of μ-CeO_2 at 40 mg/L shows a small feature of Ce(III) oxidation state (2.9 ± 0.2%), suggesting a small extent of transformation. However, the feature of Ce(III) under n-CeO_2 (40 mg/L) account for 12.8 ± 2.3% of the total Ce. This is equivalent to a release of 5.96 mg/kg (46.5 × 12.8%) Ce^{3+} in planarian, which demonstrated our hypothesis that biotransformation contributed to the toxicity observed for n-CeO_2. It should be also noted that the concentration of Ce(III) is twice of that in Ce^{3+} treated group (2.8 mg/kg), while the toxicity is lower than Ce^{3+}. This can be attributed to the fact that the biotransformation of nanomaterials is a time-dependent process. For example, it can take up to 7 days to show 20% of transformation of n-CeO_2 in plant shoot[57]. Depending on different species, the transformation rate can be lower or higher. Unlike Ce^{3+} which instantly release all the Ce^{3+} to organism and thus cause acute toxicity, n-CeO_2 released Ce^{3+} slowly by continuously interact with the planarian thus the toxicity is more chronic rather than acute. As with all chemicals and bulk materials, the biological and/or toxicological effects of NPs will be affected by both their physicochemical properties and the biological environment around the organism. NPs interactions with biological environments result in the formation of a protein corona[58, 59]. A corona-NPs complex may feature NPs undergoing different changes as a result of their adsorption behavior, agglomeration, accumulation, distribution, biotransformation, and dissolution. A protein corona complex and NPs represent a new entity in every biological environment which will inevitably define NPs toxicology, pharmacokinetics, and dynamics[60, 61]. In the present study, we found that n-CeO_2 induced a more mucus secreted by planarian and the higher biotransformation occurred with a higher toxicity in the homeostatic and regeneration planarians. In fact, n-CeO_2 would gain a negative charge due to the formation of a protein-corona-NPs complex and cause planarian absorbed a more n-CeO_2, which may promote NPs' biotransformation and dissolution (**Fig. S7**, **Table. S4**). Thus, we hypothesized that the protein corona affects not only n-CeO_2's distribution, but also its toxicity. In summary, n-CeO_2 induced toxicity to planarian via both its nano-specific effect as well as the ions induced effects.

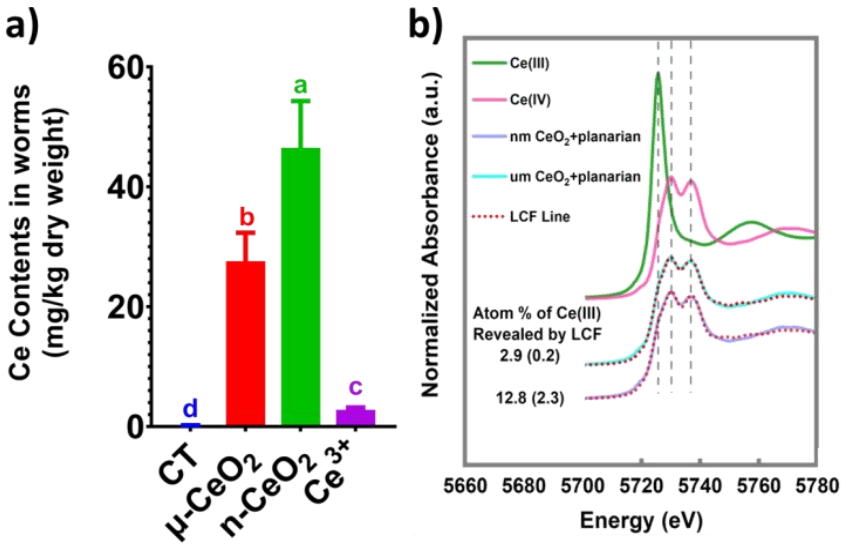

Fig. 3 a) Cerium contents in the regeneration planarians at 2 dpa in different treatments. Data are expressed as mean ±SD (n=6) an average of six replicates. Different letters stand for statistical differences between treatments at $p<0.05$. **b)** XANES normalized Ce L_{III}-edge spectra of reference compounds ($CePO_4$ and CeO_2) and samples. μ-CeO_2, n-CeO_2 and Ce^{3+} ions exposure to regeneration planarians for 2 days and the samples were detected by XANES. Ce speciation in Ce^{3+} treatment sample could not be detected, as the Ce signal was too low to obtain a reliable spectrum.

3.4 n-CeO_2 disrupts the antioxidant system and damage DNA integrity

In previous studies, Ce^{3+}/Ce^{4+} fractions (two reversible states) on n-CeO_2 particle surfaces were found to determine the particle's SOD mimicking activity[62]. Compared with the smaller n-CeO_2, n-CeO_2 with dimensions bigger than 5 nm exhibit a lower Ce^{3+}/Ce^{4+} ratio, and thus exhibit negligible activity[63]. Once n-CeO_2 undergoes biotransformation and releases Ce^{3+} ions, which plays a role of pro-oxidative effects, and the toxicity would be exhibited[24]. In addition, a Fenton-like reaction could be catalyzed by the released Ce^{3+} ions with hydrogen peroxide, producing damaging oxygen radicals, which may cause oxidative stress happened[64]. Oxidative stress has been considered a major contributor to the toxicity of environmental pollutants including nanomaterials[65-67]. Changes in activities of antioxidant enzymes and contents of MDA are the primary indicators of oxidative stress and cell damage. The antioxidant enzymes such as SOD, GPX, and GST, are involved in the protective mechanisms adapted by animals to scavenge ROS[68]. To examine whether the disorder of redox balance underlies the toxicity of n-CeO_2, we evaluated the expression levels of different categories of antioxidative in regeneration planarians. In this study, the antioxidant defense system including enzymatic (SOD, GST and GPx) and non-enzymatic (GSH, GSSG) and MDA levels were

determined in the regenerating planarians. As shown in **Fig. 4a-c**, both n-CeO_2 and Ce^{3+} treatments induced significant changes in the activities of SOD, GST, and GPx in planarians. n-CeO_2 and Ce^{3+} decreased the activity of SOD by 28.6% and 34.4%, respectively, compared with CT. The activity of GST in planarians in n-CeO_2 and Ce^{3+} treatment was significantly decreased as compared to that of CT. n-CeO_2 and Ce^{3+} significantly decreased the GPx activity by 38.8% and 37.5%, respectively. The results of the present study indicate that both n-CeO_2 and Ce^{3+} treatments disturbed the homeostasis of antioxidant defense system in regeneration planarians. A similar pattern of impacts on the non-enzymatic antioxidant system was also observed (**Fig. 4d** and **4e**). The GSH contents at 2 dpa decreased by 26.8% and 32.1 % after exposure to n-CeO_2 and Ce^{3+}, respectively. Correspondingly, a significant increase of the GSSG content, an oxidized from of GSH, was observed in planarians after exposure to n-CeO_2 and Ce^{3+}. n-CeO_2 and Ce^{3+} decreased activities of SOD, GST, GPx and GSH in the regeneration planarians compared to control with a higher level of MDA and GSSG which suggests the treatments provoked lipid peroxidation.

We further examined whether the antioxidant system was impaired at the genetic level by examining the mRNA expression of key genes responsible for antioxidant production (*gpx*, *gst*), ATP synthesis (*nak*), and cell apoptosis (*p53*) (**Fig. 5**). Consistent with the above result, *gpx*, *gst*, and *nak* expression were significantly down-regulated after 2 days of exposure to n-CeO_2 and Ce^{3+}. μ-CeO_2 did not show significant difference with CT in all cases. *Gpx* and *gr* are key antioxidant defense genes involved in the glutathione metabolism. In planarians, *p53* has a wider range of functions than known tumor suppressor[69]. Pearson and Alvarado [70] found that *p53* involved in tumor inhibition and regulation of stem cell self-renewal in planarians. In this work, *p53* expression was significantly up-regulated under n-CeO_2 and Ce^{3+} exposure when compared with CT. The apoptosis was affected in regenerating planarians, which could be due to the ability of Ce^{3+} to promote programmed cell death.

Oxidative stress can cause tissue alternations, trigger apoptosis and induce cell death. So we studied whether n-CeO_2 and Ce^{3+} exposure can induce cell apoptosis (**Fig. 4g**) and DNA damage at the molecular levels (**Fig. 4h**). 8-OHdG, a maker for oxidative DNA damage, was increased after n-CeO_2 and Ce^{3+} exposure (**Fig. 4h**), indicating n-CeO_2 and Ce^{3+} exposure can cause genotoxic effects Similarly, Arslan, et al. [71] found 0.78 mg/L n-CeO_2 induced genotoxic effect *in vitro* using micronucleus and chromosome aberration tests.

The overall oxidative responses of planarian to n-CeO_2 and Ce^{3+} are similar and to similar extents on molecular level (**Fig. 5**), although the phenotypic effects caused by the two are different. Since the phenotypic changes are essentially originated from the changes at molecular or genetic levels and given that n-CeO_2 can release toxic Ce^{3+} in a slow and sustained way, these findings give implications that n-CeO_2 may cause longer-term adverse impacts to planarian, which might be worse than that caused by acute exposure to Ce^{3+}.

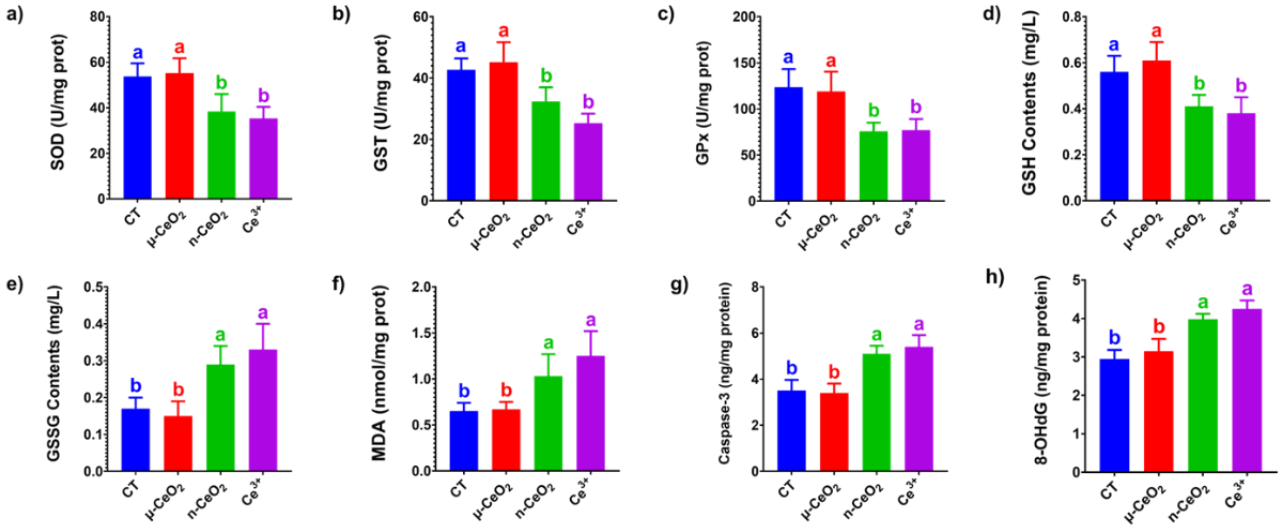

Fig. 4 n-CeO_2 regulates planarian's antioxidant defense system and cell damage. SOD (**a**), GST (**b**), GPx (**c**), GSH (**d**), GSSG (**e**), and MDA levels (**f**) in regeneration planarians after exposure to Ce-based suspensions for 48 h. Contents of caspase-3 (**g**) and 8-OHdG (**h**) in planarians affected by Ce-based suspensions treatments. Different letters stand for statistical differences between treatments at $p<0.05$.

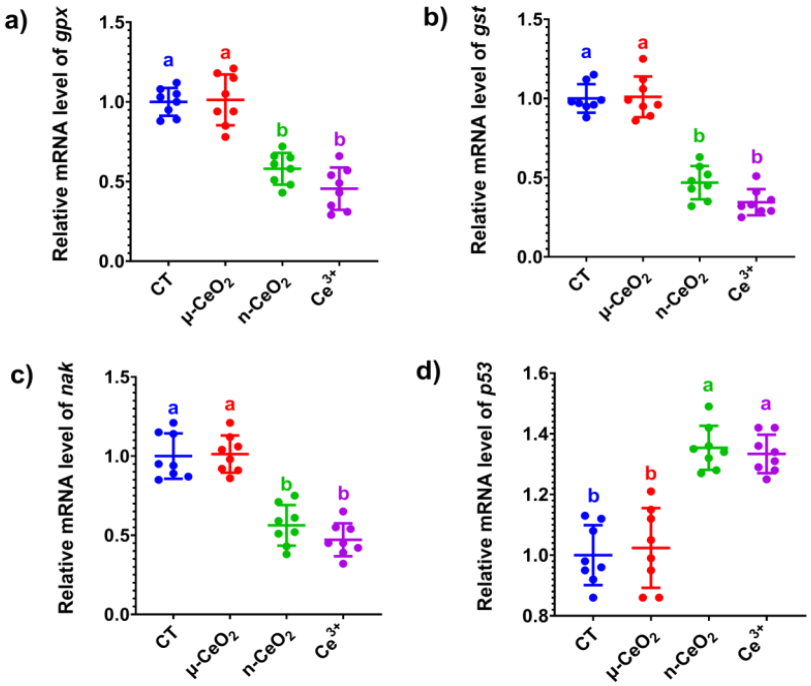

Fig. 5 The effect of Ce-based suspensions on relative mRNA expression levels of gene *gpx* (**a**), *gst* (**b**), *nak* (**c**), and *p53* (**d**) measured in regeneration planarians. Different letters stand for statistical differences between treatments at $p<0.05$.

4. Conclusion

In this study we compared the toxicity effects of n-CeO_2, μ-CeO_2, and ionic Ce ($CeCl_3$) in planarian *D. japonica*. We not only showed that n-CeO_2 induced nano-specific toxicity to planarian compared with μ-CeO_2, but also demonstrated that the biotransformation of n-CeO_2 contributed significantly to the observed toxicity. Interestingly, although n-CeO_2 induced more Ce accumulation in the planarians than Ce^{3+}, the toxicity is actually lower which is attributed to that the release of Ce^{3+} from n-CeO_2 is a slow process. However, this in turn implicates that n-CeO_2 may cause long-term adverse effects to planarian, especially to the regenerating ones which are more sensitive to the n-CeO_2 toxicity. This knowledge gap should be addressed in the future. On the other hand, interests in exploring the beneficial effects of n-CeO_2 to enhance regeneration of neural systems have increasingly growing due to the ROS capturing activity of n-CeO_2. However, such effects are only reported at very low concentrations and particles with extremely small size (usually less than 10 nm). Our results suggest that a threshold between an inhibitor and an enhancer should be established, and caution should be made for this type of application.

CRediT authorship contribution statement

Changjian Xie: Conceptualization, Methodology, Investigation, Formal analysis, Writing-original draft, Funding acquisition. **Xiaowei Li:** Methodology, Resources. **Lisha Hei:** Resources, review & editing. **Yiqing Chen:** Resources, review & editing. **Yuling Dong:** Investigation, Funding acquisition. **Shujing Zhang**: Resources. **Shan Ma:** Investigation. **Jianing Xu:** Formal analysis, Funding acquisition**. Qiuxiang Pang:** Conceptualization, Methodology, Formal analysis, Writing-review & editing, Resources. **Iseult Lynch:** Funding acquisition, Writing-review & editing. **Zhiling Guo:** Conceptualization, Methodology, Formal analysis, Writing-review & editing, Resources. **Peng Zhang:** Writing-review & editing, Resources.

Declaration of competing interest

The authors declare that they have no competing interests.

Acknowledgments

This work was supported by the National Natural Science Foundation of China (Grant Nos. 12105163, 32001987) and the Natural Science Foundation of Shandong Province (Grant Nos. ZR2020QD133, ZR2020QC241, ZR2020MC142). Additional support from H2020 project NanoCommons (Grant Agreement No. 731032) is acknowledged.

References

1. Keller, A. A.; McFerran, S.; Lazareva, A.; Suh, S. J. J. o. n. r., Global life cycle releases of engineered nanomaterials. **2013,** *15*, (6), 1-17.
2. Dahle, J. T.; Arai, Y. J. I. j. o. e. r.; health, p., Environmental geochemistry of cerium: applications and toxicology of cerium oxide nanoparticles. **2015,** *12*, (2), 1253-1278.
3. Das, S.; Dowding, J. M.; Klump, K. E.; McGinnis, J. F.; Self, W.; Seal, S. J. N., Cerium oxide nanoparticles: applications and prospects in nanomedicine. **2013,** *8*, (9), 1483-1508.
4. Hoecke, K. V.; Quik, J. T.; Mankiewicz-Boczek, J.; Schamphelaere, K. A. D.; Elsaesser, A.; Meeren, P. V. d.; Barnes, C.; McKerr, G.; Howard, C. V.; Meent, D. V. D. J. E. s.; technology, Fate and effects of CeO2 nanoparticles in aquatic ecotoxicity tests. **2009,** *43*, (12), 4537-4546.
5. Leynen, N.; Van Belleghem, F. G.; Wouters, A.; Bove, H.; Ploem, J.-P.; Thijssen, E.; Langie, S. A.; Carleer, R.; Ameloot, M.; Artois, T. J. N., In vivo toxicity assessment of silver nanoparticles in homeostatic versus regenerating planarians. **2019,** *13*, (4), 476-491.
6. Chen, J.; Patil, S.; Seal, S.; McGinnis, J. F. J. N. n., Rare earth nanoparticles prevent retinal degeneration induced by intracellular peroxides. **2006,** *1*, (2), 142-150.
7. Li, Y.; He, X.; Yin, J. J.; Ma, Y.; Zhang, P.; Li, J.; Ding, Y.; Zhang, J.; Zhao, Y.; Chai, Z. J. A. C., Acquired superoxide‐scavenging ability of ceria nanoparticles. **2015,** *127*, (6), 1852-1855.

8. Lee, S. S.; Song, W.; Cho, M.; Puppala, H. L.; Nguyen, P.; Zhu, H.; Segatori, L.; Colvin, V. L. J. A. n., Antioxidant properties of cerium oxide nanocrystals as a function of nanocrystal diameter and surface coating. **2013,** *7*, (11), 9693-9703.
9. Pirmohamed, T.; Dowding, J. M.; Singh, S.; Wasserman, B.; Heckert, E.; Karakoti, A. S.; King, J. E.; Seal, S.; Self, W. T. J. C. c., Nanoceria exhibit redox state-dependent catalase mimetic activity. **2010,** *46*, (16), 2736-2738.
10. Popov, A. L.; Popova, N. R.; Selezneva, I. I.; Akkizov, A. Y.; Ivanov, V. K. J. M. S.; C, E., Cerium oxide nanoparticles stimulate proliferation of primary mouse embryonic fibroblasts in vitro. **2016,** *68*, 406-413.
11. Popov, A.; Ermakov, A.; Savintseva, I.; Selezneva, I.; Poltavtseva, R.; Zaraisky, E.; Poltavtsev, A.; Stepanov, A.; Ivanov, V.; Sukhikh, G., Citrate-stabilized nanoparticles of ceo 2 stimulate proliferation of human mesenchymal stem cells in vitro. *Nanoscience and Technology: An International Journal* **2016,** *7*, (3).
12. Singh, R.; Karakoti, A. S.; Self, W.; Seal, S.; Singh, S. J. L., Redox-sensitive cerium oxide nanoparticles protect human keratinocytes from oxidative stress induced by glutathione depletion. **2016,** *32*, (46), 12202-12211.
13. Zhang, H.; He, X.; Zhang, Z.; Zhang, P.; Li, Y.; Ma, Y.; Kuang, Y.; Zhao, Y.; Chai, Z. J. E. s.; technology, Nano-CeO2 exhibits adverse effects at environmental relevant concentrations. **2011,** *45*, (8), 3725-3730.
14. Xie, C.; Ma, Y.; Zhang, P.; Zhang, J.; Li, X.; Zheng, K.; Li, A.; Wu, W.; Pang, Q.; He, X., Elucidating the origin of the toxicity of nano-CeO 2 to Chlorella pyrenoidosa: the role of specific surface area and chemical composition. *Environmental Science: Nano* **2021,** *8*, 1701-1712.
15. Rossbach, L. M.; Brede, D. A.; Nuyts, G.; Cagno, S.; Olsson, R. M. S.; Oughton, D. H.; Falkenberg, G.; Janssens, K.; Lind, O. C., Synchrotron XRF Analysis Identifies Cerium Accumulation Colocalized with Pharyngeal Deformities in CeO2 NP-Exposed Caenorhabditis elegans. *Environmental Science & Technology* **2022,** *56*, (8), 5081-5089.
16. Kuang, Y.; He, X.; Zhang, Z.; Li, Y.; Zhang, H.; Ma, Y.; Wu, Z.; Chai, Z. J. J. o. n.; nanotechnology, Comparison study on the antibacterial activity of nano-or bulk-cerium oxide. **2011,** *11*, (5), 4103-4108.
17. Manier, N.; Bado-Nilles, A.; Delalain, P.; Aguerre-Chariol, O.; Pandard, P. J. E. p., Ecotoxicity of non-aged and aged CeO2 nanomaterials towards freshwater microalgae. **2013,** *180*, 63-70.
18. Sendra, M.; Yeste, P.; Moreno-Garrido, I.; Gatica, J. M.; Blasco, J. J. S. o. T. T. E., CeO2 NPs, toxic or protective to phytoplankton? Charge of nanoparticles and cell wall as factors which cause changes in cell complexity. **2017,** *590*, 304-315.
19. Alabresm, A.; Decho, A. W.; Lead, J. J. N., A novel method to estimate cellular internalization of nanoparticles into gram-negative bacteria: Non-lytic removal of outer membrane and cell wall. **2021,** *21*, 100283.
20. Bour, A.; Mouchet, F.; Verneuil, L.; Evariste, L.; Silvestre, J.; Pinelli, E.; Gauthier, L. J. C., Toxicity of CeO2 nanoparticles at different trophic levels–effects on diatoms, chironomids and amphibians. **2015,** *120*, 230-236.
21. Yang, X.; Pan, H.; Wang, P.; Zhao, F.-J. J. J. o. H. M., Particle-specific toxicity and bioavailability of cerium oxide (CeO2) nanoparticles to Arabidopsis thaliana. **2017,** *322*, 292-300.
22. Bandyopadhyay, S.; Peralta-Videa, J. R.; Plascencia-Villa, G.; José-Yacamán, M.; Gardea-Torresdey, J. L. J. J. o. h. m., Comparative toxicity assessment of CeO2 and ZnO nanoparticles towards Sinorhizobium meliloti, a symbiotic alfalfa associated bacterium: use of advanced microscopic and spectroscopic techniques. **2012,** *241*, 379-386.
23. Zhang, P.; Ma, Y.; Zhang, Z.; He, X.; Zhang, J.; Guo, Z.; Tai, R.; Zhao, Y.; Chai, Z., Biotransformation of ceria nanoparticles in cucumber plants. *ACS nano* **2012,** *6*, (11), 9943-9950.
24. Xie, C.; Zhang, J.; Ma, Y.; Ding, Y.; Zhang, P.; Zheng, L.; Chai, Z.; Zhao, Y.; Zhang, Z.; He, X., Bacillus subtilis causes dissolution of ceria nanoparticles at the nano–bio interface. *Environmental Science: Nano* **2019,** *6*, (1), 216-223.
25. Thill, A.; Zeyons, O.; Spalla, O.; Chauvat, F.; Rose, J.; Auffan, M.; Flank, A. M. J. E. s.; technology, Cytotoxicity of CeO2 nanoparticles for Escherichia coli. Physico-chemical insight of the cytotoxicity mechanism. **2006,** *40*, (19), 6151-6156.
26. Leynen, N.; Van Belleghem, F. G.; Wouters, A.; Bove, H.; Ploem, J.-P.; Thijssen, E.; Langie, S. A.; Carleer, R.; Ameloot,

M.; Artois, T., In vivo toxicity assessment of silver nanoparticles in homeostatic versus regenerating planarians. *Nanotoxicology* **2019,** *13*, (4), 476-491.
27. Kluever, A. N.; Aungst, J.; Gu, Y.; Hatwell, K.; Shackelford, M., Infant toxicology: State of the science and considerations in evaluation of safety. *Food. Chem. Toxicol* **2014,** *70*, (2), 68-83.
28. Perera, F.; Herbstman, J., Prenatal environmental exposures, epigenetics, and disease. *Reprod. Toxicol* **2011,** *31*, (3), 363-373.
29. Zeng, A.; Li, H.; Guo, L.; Gao, X.; McKinney, S.; Wang, Y.; Yu, Z.; Park, J.; Semerad, C.; Ross, E. J. C., Prospectively isolated tetraspanin+ neoblasts are adult pluripotent stem cells underlying planaria regeneration. **2018,** *173*, (7), 1593-1608. e20.
30. Dong, Z.; Huo, J.; Liang, A.; Chen, J.; Chen, G.; Liu, D., Gamma-Secretase Inhibitor (DAPT), a potential therapeutic target drug, caused neurotoxicity in planarian regeneration by inhibiting Notch signaling pathway. *Science of The Total Environment* **2021,** *781*, 146735.
31. Morris, J.; Bealer, E. J.; Souza, I. D.; Repmann, L.; Bonelli, H.; Stanzione III, J. F.; Staehle, M. M. J. T. S., Chemical Exposure-Induced Developmental Neurotoxicity in Head-Regenerating Schmidtea mediterranea. **2022,** *185*, (2), 220-231.
32. Zhang; Jianyong; Bin; Wang; Bosheng; Zhao; Yanqing; Li; Xiuyun; Pollution, Z. J. E., Blueberry anthocyanin alleviate perfluorooctanoic acid-induced toxicity in planarian (Dugesia japonica) by regulating oxidative stress biomarkers, ATP contents, DNA methylation and mRNA expression. **2019**.
33. Rompolas, P.; Patel-King, R. S.; King, S. M., Schmidtea mediterranea: a model system for analysis of motile cilia. In *Methods in cell biology*, Elsevier: 2009; Vol. 93, pp 81-98.
34. Gao, T.; Sun, B.; Xu, Z.; Chen, Q.; Yang, M.; Wan, Q.; Song, L.; Chen, G.; Jing, C.; Zeng, E. Y. J. J. o. H. M., Exposure to polystyrene microplastics reduces regeneration and growth in planarians. **2022,** *432*, 128673.
35. Gambino, G.; Falleni, A.; Nigro, M.; Salvetti, A.; Cecchettini, A.; Ippolito, C.; Guidi, P.; Rossi, L. J. A. T., Dynamics of interaction and effects of microplastics on planarian tissue regeneration and cellular homeostasis. **2020,** *218*, 105354.
36. Tran, T. A.; Hesler, M.; Moriones, O. H.; Jimeno-Romero, A.; Fischer, B.; Bastús, N. G.; Puntes, V.; Wagner, S.; Kohl, Y. L.; Gentile, L. J. A.-A. t. a. e., Assessment of iron oxide nanoparticle ecotoxicity on regeneration and homeostasis in the replacement model system Schmidtea mediterranea. **2019,** *36*, (4), 583-596.
37. Kustov, L.; Tiras, K.; Al-Abed, S.; Golovina, N.; Ananyan, M. J. A. t. L. A., Estimation of the toxicity of silver nanoparticles by using planarian flatworms. **2014,** *42*, (1), 51-58.
38. Ermakov, A.; Popov, A.; Ermakova, O.; Ivanova, O.; Baranchikov, A.; Kamenskikh, K.; Shekunova, T.; Shcherbakov, A.; Popova, N.; Ivanov, V., The first inorganic mitogens: Cerium oxide and cerium fluoride nanoparticles stimulate planarian regeneration via neoblastic activation. *Mater. Sci. Eng. C* **2019,** *104*, 109924.
39. Zhang, P.; Ma, Y.; Zhang, Z.; He, X.; Li, Y.; Zhang, J.; Zheng, L.; Zhao, Y. J. N., Species-specific toxicity of ceria nanoparticles to Lactuca plants. **2015,** *9*, (1), 1-8.
40. Rui, Y.; Zhang, P.; Zhang, Y.; Ma, Y.; He, X.; Gui, X.; Li, Y.; Zhang, J.; Zheng, L.; Chu, S. J. E. P., Transformation of ceria nanoparticles in cucumber plants is influenced by phosphate. **2015,** *198*, 8-14.
41. Ermakov, A.; Popov, A.; Ermakova, O.; Ivanova, O.; Baranchikov, A.; Kamenskikh, K.; Shekunova, T.; Shcherbakov, A.; Popova, N.; Ivanov, V., The first inorganic mitogens: Cerium oxide and cerium fluoride nanoparticles stimulate planarian regeneration via neoblastic activation. *Materials Science and Engineering: C* **2019,** *104*, 109924.
42. Shibata, N.; Rouhana, L.; Agata, K. J. D., growth; differentiation, Cellular and molecular dissection of pluripotent adult somatic stem cells in planarians. **2010,** *52*, (1), 27-41.
43. Gao, L.; Li, A.; Lv, Y.; Huang, M.; Liu, X.; Deng, H.; Liu, D.; Zhao, B.; Liu, B.; Pang, Q., Planarian gamma-interferon-inducible lysosomal thiol reductase (GILT) is required for gram-negative bacterial clearance. *Developmental & Comparative Immunology* **2021,** *116*, 103914.

44. Dong, Z.; Cheng, F.; Yang, Y.; Zhang, F.; Chen, G.; Liu, D., Expression and functional analysis of flotillins in Dugesia japonica. *Experimental cell research* **2019,** *374*, (1), 76-84.
45. Collin, B.; Oostveen, E.; Tsyusko, O. V.; Unrine, J. M. J. E. s.; technology, Influence of natural organic matter and surface charge on the toxicity and bioaccumulation of functionalized ceria nanoparticles in Caenorhabditis elegans. **2014,** *48*, (2), 1280-1289.
46. Lobo, D.; Beane, W. S.; Levin, M. J. P. c. b., Modeling planarian regeneration: a primer for reverse-engineering the worm. **2012,** *8*, (4), e1002481.
47. Perera, F.; Herbstman, J. J. R. t., Prenatal environmental exposures, epigenetics, and disease. **2011,** *31*, (3), 363-373.
48. Matson, J. P.; Cook, J. G. J. T. F. j., Cell cycle proliferation decisions: the impact of single cell analyses. **2017,** *284*, (3), 362-375.
49. González-Estévez, C.; Felix, D. A.; Aboobaker, A. A.; Saló, E. J. P. o. t. N. A. o. S., Gtdap-1 promotes autophagy and is required for planarian remodeling during regeneration and starvation. **2007,** *104*, (33), 13373-13378.
50. Brown, D. D.; Pearson, B. J. J. F. i. n., A brain unfixed: unlimited neurogenesis and regeneration of the adult planarian nervous system. **2017,** *11*, 289.
51. Umesono, Y.; Watanabe, K.; Agata, K., Distinct structural domains in the planarian brain defined by the expression of evolutionarily conserved homeobox genes. *Development genes and evolution* **1999,** *209*, (1), 31-39.
52. Cui, D.; Zhang, P.; Ma, Y.; He, X.; Li, Y.; Zhang, J.; Zhao, Y.; Zhang, Z. J. E. S. N., Effect of cerium oxide nanoparticles on asparagus lettuce cultured in an agar medium. **2014,** *1*, (5), 459-465.
53. Ding, X.; Pu, Y.; Tang, M.; Zhang, T. J. N. T., Environmental and health effects of graphene-family nanomaterials: potential release pathways, transformation, environmental fate and health risks. **2022,** *42*, 101379.
54. Ding, L.; Liu, Z.; Okweesi Aggrey, M.; Li, C.; Chen, J.; Tong, L., Nanotoxicity: the toxicity research progress of metal and metal-containing nanoparticles. *Mini reviews in medicinal chemistry* **2015,** *15*, (7), 529-542.
55. Guo, Z.; Zhang, P.; Chakraborty, S.; Chetwynd, A. J.; Abdolahpur Monikh, F.; Stark, C.; Ali-Boucetta, H.; Wilson, S.; Lynch, I.; Valsami-Jones, E., Biotransformation modulates the penetration of metallic nanomaterials across an artificial blood–brain barrier model. *Proceedings of the National Academy of Sciences* **2021,** *118*, (28), e2105245118.
56. Zhang, P.; Guo, Z.; Zhang, Z.; Fu, H.; White, J. C.; Lynch, I., Nanomaterial transformation in the soil–plant system: implications for food safety and application in agriculture. *Small* **2020,** *16*, (21), 2000705.
57. Ma, Y.; Zhang, P.; Zhang, Z.; He, X.; Zhang, J.; Ding, Y.; Zhang, J.; Zheng, L.; Guo, Z.; Zhang, L. J. E. s.; technology, Where does the transformation of precipitated ceria nanoparticles in hydroponic plants take place? **2015,** *49*, (17), 10667-10674.
58. Docter, D.; Westmeier, D.; Markiewicz, M.; Stolte, S.; Knauer, S.; Stauber, R. J. C. S. R., The nanoparticle biomolecule corona: lessons learned–challenge accepted? **2015,** *44*, (17), 6094-6121.
59. Lane, L. A.; Qian, X.; Smith, A. M.; Nie, S. J. A. r. o. p. c., Physical Chemistry of Nanomedicine: Understanding the Complex Behaviors of Nanoparticles In-Vivo. **2015,** *66*, 521.
60. Fleischer, C. C.; Payne, C. K. J. A. o. c. r., Nanoparticle–cell interactions: molecular structure of the protein corona and cellular outcomes. **2014,** *47*, (8), 2651-2659.
61. Walczyk, D.; Bombelli, F. B.; Monopoli, M. P.; Lynch, I.; Dawson, K. A. J. J. o. t. A. C. S., What the cell "sees" in bionanoscience. **2010,** *132*, (16), 5761-5768.
62. Wei, H.; Wang, E. J. C. S. R., Nanomaterials with enzyme-like characteristics (nanozymes): next-generation artificial enzymes. **2013,** *42*, (14), 6060-6093.
63. Dowding, J. M.; Das, S.; Kumar, A.; Dosani, T.; McCormack, R.; Gupta, A.; Sayle, T. X.; Sayle, D. C.; von Kalm, L.; Seal, S. J. A. n., Cellular interaction and toxicity depend on physicochemical properties and surface modification of redox-active nanomaterials. **2013,** *7*, (6), 4855-4868.

64. Rico, C. M.; Johnson, M. G.; Marcus, M. A. J. E. S. N., Cerium oxide nanoparticles transformation at the root–soil interface of barley (Hordeum vulgare L.). **2018,** *5*, (8), 1807-1812.
65. Limbach, L. K.; Wick, P.; Manser, P.; Grass, R. N.; Bruinink, A.; Stark, W. J. J. E. s.; technology, Exposure of engineered nanoparticles to human lung epithelial cells: influence of chemical composition and catalytic activity on oxidative stress. **2007,** *41*, (11), 4158-4163.
66. Gong, X.; Huang, D.; Liu, Y.; Zeng, G.; Wang, R.; Wan, J.; Zhang, C.; Cheng, M.; Qin, X.; Xue, W. J. E. s.; technology, Stabilized nanoscale zerovalent iron mediated cadmium accumulation and oxidative damage of Boehmeria nivea (L.) Gaudich cultivated in cadmium contaminated sediments. **2017,** *51*, (19), 11308-11316.
67. Ma, Y.; Xie, C.; He, X.; Zhang, B.; Yang, J.; Sun, M.; Luo, W.; Feng, S.; Zhang, J.; Wang, G., Effects of Ceria Nanoparticles and CeCl3 on Plant Growth, Biological and Physiological Parameters, and Nutritional Value of Soil Grown Common Bean (Phaseolus vulgaris). *Small* **2020**, 1907435.
68. Yang, J.; Cao, W.; Rui, Y., Interactions between nanoparticles and plants: phytotoxicity and defense mechanisms. *Journal of Plant Interactions* **2017,** *12*, (1), 158-169.
69. Van Roten, A.; Barakat, A. Z. A.-Z.; Wouters, A.; Tran, T. A.; Mouton, S.; Noben, J.-P.; Gentile, L.; Smeets, K., A carcinogenic trigger to study the function of tumor suppressor genes in Schmidtea mediterranea. *Disease models & mechanisms* **2018,** *11*, (9), dmm032573.
70. Pearson, B. J.; Alvarado, A. S. J. D., A planarian p53 homolog regulates proliferation and self-renewal in adult stem cell lineages. **2010,** *137*, (2), 213-221.
71. Arslan, K.; Akbaba, G. B. J. T.; Health, I., In vitro genotoxicity assessment and comparison of cerium (IV) oxide micro-and nanoparticles. **2020,** *36*, (2), 76-83.